Comparisons of Experimental and FEA Results in Ultrasonic- and MQL-assisted Machining of Titanium Alloy

Erkin Duman
Istanbul Gedik University, Kartal, Istanbul, Türkiye

Yusuf Furkan Yapan
Yildiz Technical University, Besiktas, Istanbul, Türkiye

Mehmet Alper Sofuoğlu
Eskisehir Osmangazi University, Odunpazari, Eskisehir, Türkiye

Alper Uysal
Yildiz Technical University, Besiktas, Istanbul, Türkiye

Abstract:

Challenges in machining Ti-6Al-7Nb titanium alloy have forced researchers to investigate new advanced machining methods. In this study, the effects of dry and minimum quantity lubrication (MQL) cutting conditions on the cutting forces and cutting temperature in conventional and ultrasonic vibration assisted turning of Ti-6Al-7Nb alloy were investigated experimentally and numerically. Ultrasonic vibration assisted MQL (UVA-MQL) method provided improvement in cutting performance compared to all other methods in terms of cutting force and cutting temperature. The experimental results and numerical results were in good agreement and the underlying reasons for the improved cutting mechanism were revealed.

Keywords:

Finite element analysis, Minimum quantity lubrication, Ti-6Al-7Nb, Ultrasonic-vibration assisted cutting.

I. Introduction

Titanium and its alloys are widely utilized in the biomedical industry due to their excellent biocompatibility, corrosion resistance, and mechanical properties [1]. Among these, Ti-6Al-7Nb has emerged as a promising alternative to the extensively used Ti-6Al-4V alloy, particularly for biomedical implants, as it eliminates the potential toxicity of vanadium while maintaining comparable mechanical and biological performance [2]. However, machining Ti-6Al-7Nb remains a significant challenge due to its low thermal conductivity, high chemical reactivity, and pronounced work hardening, leading to excessive tool wear and surface integrity issues [3].

Traditional dry machining of titanium alloys often results in elevated cutting temperatures and high cutting forces, which adversely affect surface integrity and tool life [4]. To mitigate these challenges, researchers have explored various advanced machining techniques, including ultrasonic vibration-assisted turning (UVAT). UVAT has been demonstrated to reduce cutting forces, enhance chip breakability, and improve surface quality by introducing periodic vibrations to the cutting tool [5]. The intermittent contact between the tool and the workpiece in UVAT effectively reduces cutting temperature and friction, leading to improved tool life and process stability [5].

In order to further improve the machinability of Ti-6Al-7Nb and to further increase the positive effect of UVAT, studies carried out under the minimum quantity lubrication (MQL) method with UVAT have started to attract attention in recent years [6]. Improvement in machining performance can be achieved due to the advantages of the methods combined under the ultrasonic vibration-assisted minimum quantity lubrication (UVA-MQL) cutting condition and the synergistic effect resulting from the interaction of the methods [7].

In addition to all these, determining the machining outputs before the process with finite element analysis (FEA) offers significant advantages in terms of optimization of manufacturing processes and cost effectiveness [8]. FEA allows critical parameters such as cutting forces, temperature distribution, tool wear, and surface integrity to be estimated through simulation [8]. In this way, process parameters can be optimized and potential problems can be predicted before starting experimental studies. In addition, understanding the cutting mechanism contributes to the development of more efficient cutting strategies by revealing the dynamics of material-tool interaction. These analyses play a critical role in improving machining performance and ensuring the reliability of manufacturing processes, especially in difficult-to-machine materials such as Ti-6Al-7Nb. A detailed understanding of the cutting mechanism and estimation of process outputs are of great importance in achieving the goal of improving machining performance.

II. Literature Review

Ultrasonic vibration-assisted turning (UVAT) is an innovative manufacturing tech-nology that offers superior machining capabilities compared to traditional turning methods. UAT provides periodic interruption of contact with the workpiece by vibrating the cutting tool at high frequency and low amplitude. This method provides successful results especially on materials with high temperature and tool wear problems such as Ti6Al4V, Nimonic 90, SiCp/Al composites and other difficult-to-machine alloys. In this literature review, the effects of UVAT on cutting forces, sur-face finish, tool wear, residual stresses and microstructural changes, cutting temperatures and hybrid applications are detailed and the finite element analysis (FEA) successes are evaluated.

In terms of cutting forces and temperatures, UVAT has demonstrated significant advantages over conventional turning. Wei et al. [9] investigated the effects of UVAT on medium-carbon steel using both experimental studies and finite element analysis (FEA), reporting a 9.4% deviation between FEA and experimental results, with a notable reduction in cutting forces. Bakhshan et al. [10] employed a particle finite element method (PFEM) to examine the influence of ultrasonic vibrations on cutting forces, revealing a reduction of 20% in cutting forces and a decrease of 29-44% in tool-chip contact length. The deviation between experimental and numerical results was found to be 6.2%. Deswal and Kant [11] analyzed the machinability of AZ31B magnesium alloys in UVAT, reporting a 69% reduction in cutting forces, a 65% decrease in thrust forces, and a 37% increase in cutting temperatures. Liu et al. [12] used computational engineering techniques to optimize cutting forces and temperatures in UVAT, reporting a 6.5% agreement between experimental and FEA results. Sun et al. [13] analyzed dual-excitation ultrasonic elliptical vibration-assisted cutting (UEVC) and observed that the intermittent contact between the tool and workpiece reduces cutting forces and facilitates chip evacuation. A discrepancy of 8.3% was found between FEA and experimental results. Kandi et al. [14] demonstrated that UVAT reduces cutting temperatures, thereby mitigating thermal damage. The discrepancy between FEA and experimental results was measured at 5.9%. Hu et al. [15] reported that UVAT decreases surface temperatures and improves surface quality in Ti6Al4V machining, with a 7.8% variation between numerical and experimental findings. Huan et al. [16] studied the ultrasonic elliptical vibration-assisted cutting of TiC-reinforced titanium matrix composites and observed a 60% reduction in cutting forces and a 17.6% decrease in cutting temperature, with a 7.8% difference between FEA and experimental results.

In terms of tool wear, UVAT has been found to prolong tool life and reduce wear. Xu et al. [17] analyzed the machining of austenitic stainless steel with UVAT through both experimental and theoretical approaches, demonstrating that specific ultrasonic amplitudes and cutting speeds significantly reduce tool wear, with a 7% discrepancy between FEA and experimental results. Zhou et al. [18] demonstrated that UVAT improves machinability by reducing tool wear in SiCp/Al composites, with an 8.9% difference between FEA and experimental findings.

Regarding surface quality, research findings indicate that UVAT significantly improves surface roughness. Wu et al. [19] analyzed surface defects in the machining of SiCp/Al composites and reported a reduction in surface roughness from 1.44 μm to 0.446 μm. The deviation between simulation and experimental results was 10.2%. Xia et al. [20] found that laser-assisted ultrasonic elliptical vibration turning (LUEVT) reduces cutting forces by 39.3% and enhances surface quality, with a 7.6% discrepancy between numerical and experimental findings. In terms of residual stresses and microstructural modifications, UVAT has demonstrated significant benefits. Ahmadpoor et al. [21] reported that UVAT transformed residual stresses by 49% into compressive stresses, thereby enhancing the fatigue life of machined components. Zhang et al. [22] examined ultrasonic elliptical vibration-assisted cutting and found thassssssst ultrasonic impacts increased grain refinement by up to 89.5%. The deviation between simulation and experimental results was 9.1%. Gamidi and Pasam [23] observed that UVAT induces higher compressive residual stresses in Ti6Al4V alloys, improving material strength. Fan et al. [24] found that UVAT reduces crack propagation, decreases surface scratches and pits, and improves surface roughness by 32%. Du et al. [25] observed that UVAT promotes more uniform chip formation, facilitates the fragmentation of SiC particles, and enhances surface quality, with a 7.2% discrepancy between numerical and experimental results.

In recent years, Hybrid UVAT applications have been explored to further enhance machining efficiency. Muhammad et al. [26] investigated hot ultrasonic-assisted turning (HUAT) in the machining of Ti-15333 alloys and reported improvements in both cutting force reduction and surface roughness. Airao et al. [27] studied hot ultrasonic-assisted turning (HUAT) and found that tool wear was reduced by 5-25%, with cutting forces also decreasing. The deviation between FEA predictions and experimental results was 6.4%. Gamidi and Pasam [23] investigated the effect of spot-cooled vibration-assisted turning (SCVAT) on residual stresses in Ti-6Al-4V alloys and found that FEA predictions deviated by 5.8% from experimental data.

III. Material and Methods

A. Experimental Section

The experimental setup used in the study presented in Figure 1 is given. Conventional and ultrasonic vibration-assisted turning (UVAT) experiments of Ti-6Al-7Nb titanium alloy were performed under dry and minimum quantity lubrication (MQL) with vegetable cutting oil cutting conditions using constant cutting speed (60 m/min) and feed value (0.05 mm/rev). The commercial cutting oil was pulverized and transmitted to the MQL system to be sent to the cutting zone using a 20 mL/h MQL flow rate. MQL nozzle with a 1 mm diameter was used in the experiments. The MQL nozzle was positioned in the cutting area at an angle of 20° and a distance of 10 mm.

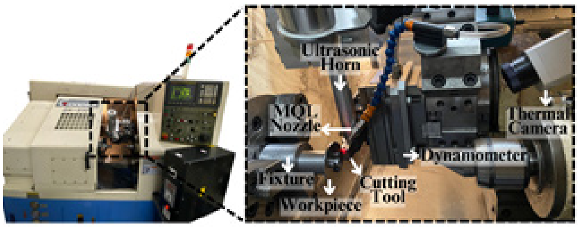

Fig. 1. Experimental setup

Turning experiments were carried out on the Goodway GA230 lathe. An uncoated tungsten carbide insert was used as the cutting tool. In order to ignore factors such as tool wear, fresh uncoated carbide inserts were used in each experiment. For UVAT experiments, vibration was applied to the cutting tool in the cutting direction with a frequency of 20 kHz and an amplitude of 20 μm. During the experiments, the cutting forces and cutting temperatures from the machining responses were measured in real-time. A Kistler dynamometer was used to measure cutting forces, while an Optris thermal camera was used to monitor cutting temperature. The experimental plan applied in the presented study is given in Table 1. As can be seen from Table 1, four different cutting conditions were investigated under constant cutting parameters (60 m/min cutting speed and 0.05 mm/rev feed value) and ultrasonic vibration parameters. Here, dry, ultrasonic vibration-assisted dry (UVA-Dry), minimum quantity lubrication (MQL), and ultrasonic vibration-assisted MQL (UVA-MQL) methods were used. As a result, cutting forces and cutting temperatures were obtained.

Table 1: Experimental and numerical analysis plan

No	Cutting Condition	Flow Rate (mL/h)	Frequency (kHz)	Amplitude (µm)
1	Dry	0	0	0
2	UVA-Dry	0	20	20
3	MQL	20	0	0
4	UVA-MQL	20	20	20

B. Finite Element Analysis Section

In the presented study, orthogonal (2D) modeling was performed using commercially available DEFORM software. The simulation was run by setting 1000 simulation steps with an implicit approach and neglecting tool wear. The boundary conditions of the orthogonal cutting finite element analysis are given in Figure 2.

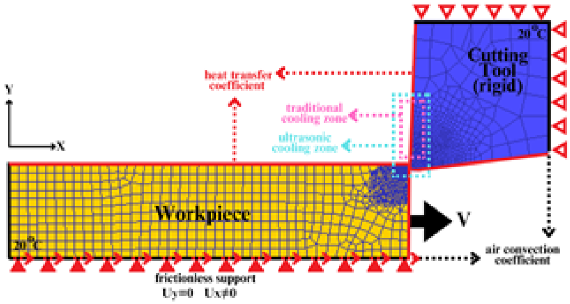

Fig. 2. Boundary conditions of the orthogonal cutting finite element analysis

The uncoated WC cutting tool with a rake angle of 2°, a clearance angle of 7° and an edge radius of 25 µm is modeled as rigid, the cutting tool is fixed, and the speed is not defined. Rectangular elements are used in meshing the cutting tool, where the total number of elements is 9743 and the number of nodes is 9963. The contact area of the cutting tool with the workpiece is more tightly meshed, this section is a critical region for modeling. The simulation is performed at room temperature. The heat transfer coefficient is defined as the edges of the cutting tool in contact with the workpiece. The edges of the cutting tool that are not in contact with the material are modeled as 20 °C.

The workpiece modeled as an isotropic elasto-plastic material is meshed with quadrilateral elements and the number of elements is 3437 and the number of nodes is 3552. Frictionless support is defined on the underside of the workpiece. This support allows the workpiece to move in the cutting direction while restricting its movement in the feed direction. The edges of the workpiece that are not in contact with the cutting tool are modeled as 20 °C. Since this part is in contact with air, a convection coefficient of 20 W/m2C is defined for this region in all simulation sets. A heat transfer coefficient of 5000 kW/m2C is assigned for the edges where the workpiece is in contact with the cutting tool. The mechanical properties of the material were obtained using JMATPRO software. The coefficients of the Johnson-Cook model were obtained by the data fitting method using the yield stress data. The Nelder-Mead Simplex method was used for the data fitting process

The characteristics of the ultrasonic vibration on the tool were defined by harmonic motion. In the simulation study, as in the experiments, 20 µm vibration amplitude and 20 kHz vibration frequency values were used. The vibration was applied in the cutting direction.

Considering that the fluid could also affect the chip and cavity surfaces of the tool due to the interrupted processing in ultrasonic-assisted machining, a wider zone was defined. Coolant heat transfer coefficients of 20000 kW/m2/C was used for the vegetable pure cutting fluid.

Friction is defined in two different regions as dry friction and dry/sliding friction. The dry friction coefficient value is assigned in the dry friction region, and the sliding friction coefficient value is assigned in the other region. In simulation studies, dry friction coefficient values are between 0.4-0.7, while sliding friction coefficient values are between 0.2-0.6.

For chip formation details, the Cockcroft & Latham model was used for chip separation. In considering this damage criterion, the shape of the chip was also taken into consideration.

IV. Results and Discussion

A. Comparison of Experimental and FEA Results

In Figure 3(a), the resultant cutting forces calculated as a result of numerical analysis are given in comparison with the experimental study. The most effective method in terms of reducing the resultant cutting force is UVA-MQL. While dry machining has the highest cutting force values, the combinations in between provide improvements at varying levels. Similar results were reported by Duman et al. [7]. It has been observed that the general trend between experimental and simulation is consistent. The experimental and numerical results of the resultant cutting force for Dry, UVA-Dry, MQL, and UVA-MQL cutting conditions had differences of 0.2%, 0.2%, 0.8%, and 2%, respectively.

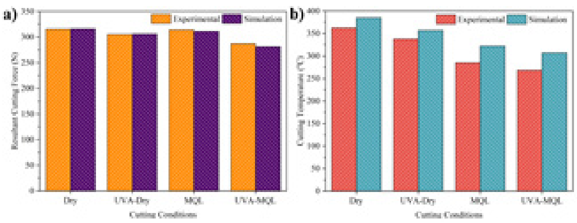

Fig. 3. Comparison of (a) resultant cutting force and (b) cutting temperature results

In Figure 3(b), the cutting temperatures calculated from FEA are given in comparison with the experimental study. The highest temperatures were observed in both data in dry machining and only in ultrasonic machining conditions. MQL and UVA-MQL significantly reduced the cutting temperatures. When UVA is included in MQL, it is seen that it is clearly superior to other methods for reducing temperature. The lowest temperature was obtained in UVA-

MQL cutting conditions. The experimental and numerical results of the cutting temperature for Dry, UVA-Dry, MQL, and UVA-MQL cutting conditions had differences of 6.4%, 5.6%, 13%, and 14.6%, respectively.

B. FEA Results for Dry vs UVA-MQL Cutting

Cutting forces, cutting temperatures and effective stresses for dry machining are given in Figure 4. As it is known from the literature [28], the force in the X direction (main cutting direction) was higher than the force in the Y direction. The temperature distribution result clearly shows that high temperatures occur at the cutting edge and chip area under dry machining conditions. Since there is no cooling/lubrication under dry machining conditions, the temperatures in the cutting area remained at higher levels. Effective stresses are concentrated around the cutting edge and in the cutting area; the highest stress values were observed at this point.

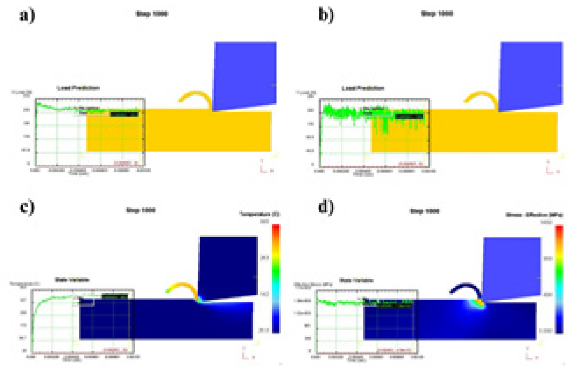

Fig. 4. (a) X-direction cutting force, (b) Y-direction cutting force, (c) Cutting temperature, (d) Effective stress for dry cutting

Cutting forces, cutting temperatures and effective stresses are given for the UVA-MQL cutting condition in Figure 5. Since the use of both ultrasonic vibration and MQL together makes the friction and chip formation in the cutting area more efficient, it is seen that the forces are lower on average compared to other cutting conditions. It can be said that the fluctuations in the graph (short-term changes up and down) are due to chip breakage during the cutting process and the interruption of cutting tool-workpiece contact by high-frequency vibration. The lubricating effect provided by the minimum amount and the chip breaking/removal advantage of ultrasonic vibration reduce friction and reduce force levels. MQL provides some cooling and lubrication at the cutting point. When the friction-reducing effect of ultrasonic vibration is added to this, a lower or more controlled temperature distribution occurs compared to dry machining or UVA-Dry machining. Although the temperature generally reaches the highest level around the cutting edge, the heat dissipation is more limited in this scenario. The stress distribution reveals that the highest values are found in the chip formation area and around the cutting edge. The stresses remain at the highest level at the first break point of the chip and at the cutting edge.

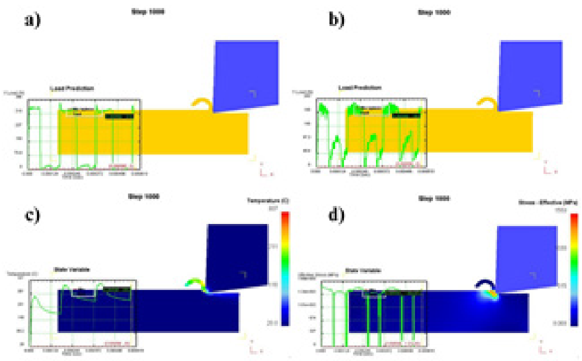

Fig. 5. (a) X-direction cutting force, (b) Y-direction cutting force, (c) Cutting temperature, (d) Effective stress for UVA-MQL

V. Conclusion

In this study, the effects of dry and minimum quantity lubrication (MQL) cutting conditions on the cutting forces and cutting temperature in conventional and ultrasonic vibration-assisted turning of Ti-6Al-7Nb alloy were investigated experimentally and numerically. The conclusions obtained are given below:

- The best cutting condition in terms of cutting temperature and resultant cutting force was obtained as UVA-MQL due to the synergistic effect between ultrasonic vibration and minimum quantity lubrication methods.
- The experimental and numerical results of the resultant cutting force for Dry, UVA-Dry, MQL, and UVA-MQL cutting conditions had differences of 0.2%, 0.2%, 0.8%, and 2%, respectively.
- The experimental and numerical results of the cutting temperature for Dry, UVA-Dry, MQL, and UVA-MQL cutting conditions had differences of 6.4%, 5.6%, 13%, and 14.6%, respectively.

VI. Acknowledgment

This study was supported by Scientific and Technological Research Council of Turkey (TUBITAK) under the Grant Number 123M048. The authors thank TUBITAK for their support.

References

1. O. Öztürk, M. Aydın, Ö. Gökcepınar, et al., "Enhancing formability of Ti-6Al-4V cylindrical cups by pulsating hydroforming process: Experimental, numerical and microstructural investigations," Eng. Sci. Technol. Int. J., vol. 50, pp. 101606, 2024.
2. M. Kaur and K. Singh, "Review on titanium and titanium based alloys as biomaterials for orthopaedic applications," Mater. Sci. Eng. C, vol. 102, pp. 844–860, 2019.
3. A. J. Festas, R. B. Pereira, A. Ramos, et al., "A study of the effect of conventional drilling and helical milling in surface quality in titanium Ti-6Al-4V and Ti-6AL-7Nb alloys for medical applications," Arabian J. Sci. Eng., vol. 46, no. 3, pp. 2361–2369, 2021.
4. X. Liang, Z. Liu, and B. Wang, "State-of-the-art of surface integrity induced by tool wear effects in machining process of titanium and nickel alloys: A review," Meas., vol. 132, pp. 150–181, 2019.
5. A. Khan, X. Wang, B. Zhao, et al., "Ultrasonic vibration-assisted cutting of titanium alloys: A state-of-the-art review," Chin. J. Aeronaut., vol. 38, no. 1, pp. 103078, 2024.

6. E. Duman, Y. F. Yapan, H. Salvi, et al., "Investigation of ultrasonic vibration assisted orthogonal turning under dry and minimum quantity lubrication conditions and performing sustainability analyses," J. Clean. Prod., vol. 434, pp. 140187, 2024.

7. E. Duman, Y. F. Yapan, A. Uysal, et al., "Ultrasonic vibration-assisted machining with minimum quantity lubrication for aerospace materials," in Adv. Manuf. Aerospace Alloys, Cham: Springer Nature Switzerland, pp. 47–76, 2024.

8. I. S. Jawahir, D. A. Stephenson, and B. Wang, "A review of advances in modeling of conventional machining processes: from merchant to the present," J. Manuf. Sci. Eng., vol. 144, pp. 110801, 2022.

9. S. Wei, P. Zou, L. Fang, et al., "Microstructure evolution of medium carbon steel during heat-assisted 3D ultrasonic vibration-assisted turning," Ultrason., vol. 135, pp. 107129, 2023.

10. H. Bakhshan, E. Oñate, and J. M. Carbonell, "Modeling of ultrasonic vibration-assisted micromachining using the particle finite element method," Comput. Part. Mech., vol. 11, pp. 2267–2290, 2024.

11. N. Deswal and R. Kant, "FE analysis of ultrasonic vibration assisted turning of magnesium AZ31B alloy," Mater. Today Proc., vol. 62, pp. 7473–7479, 2022.

12. Q. Liu, T. Hu, and W. Liu, "Research on ultrasonic vibration cutting performance based on computer-aided engineering," in 2024 Int. Conf. Electr. Drives, Power Electron. Eng. (EDPEE), Athens, Greece, pp. 283–288, 2024.

13. J. Sun, P. Li, K. Wang, et al., "Research on ultrasonic elliptical vibration-assisted cutting system based on double excitation," Int. J. Adv. Manuf. Technol., vol. 133, pp. 1379–1391, 2024.

14. R. Kandi, S. K. Sahoo, and A. K. Sahoo, "Ultrasonic vibration-assisted turning of titanium alloy Ti–6Al–4V: Numerical and experimental investigations," J. Braz. Soc. Mech. Sci. Eng., vol. 42, pp. 399, 2020.

15. K. Hu, S.-L. Lo, H. Wu, et al., "Study on influence of ultrasonic vibration on the ultra-precision turning of Ti6Al4V alloy based on simulation and experiment," IEEE Access, vol. 7, pp. 33640–33651, 2019.

16. H. Huan, W. Xu, B. Zhao, et al., "Simulation study of ultrasonic elliptical vibration cutting of TiC particle-reinforced titanium matrix composites," Metals, vol. 12, pp. 1769, 2022.

17. Y. Xu, J. Zhang, Q. Zhang, et al., "Theoretical and experimental investigations of tool wear in ultrasonic vibration–assisted turning of 304 austenitic stainless steel," Int. J. Adv. Manuf. Technol., vol. 127, pp. 3157–3181, 2023.

18. Y. Zhou, Y. Gu, J. Lin, et al., "Finite element analysis and experimental study on the cutting mechanism of SiCp/Al composites by ultrasonic vibration-assisted cutting," Ceram. Int., vol. 48, no. 23, pp. 35406–35421, 2022.

19. Q. Wu, Y. Du, Y. Yang, et al., “Simulation and experimental analysis of surface defect formation of SiCp/Al composites during ultrasonic vibration-assisted cutting,” J. Mater. Eng. Perform., 2024.

20. C. Xia, J. Lin, M. Lu, et al., “Finite element analysis and experimental study on the cutting mechanism of SiCp/Al composite in laser ultrasonic elliptic vibration turning,” Mater. Today Commun., vol. 41, pp. 110389, 2024.

21. S. S. Ahmadpoor, M. Khajehzadeh, and M. R. Razfar, “Finite element simulation and experimental investigation of machining induced residual stresses in ultrasonic elliptical vibration-assisted turning,” Mach. Sci. Technol., vol. 26, no. 3, pp. 377–395, 2022.

22. W. Zhang, J. Zhang, and Z. Wang, “Promoted grain refinement in tool-chip interface during ultrasonic elliptical vibration-assisted cutting of polycrystalline copper,” Int. J. Adv. Manuf. Technol., vol. 134, pp. 3925–3936, 2024.

23. K. Gamidi and V. K. Pasam, “Analysis of residual stresses in spot cooled vibration assisted turning of Ti6Al4V alloy using computational fluid dynamics-aided finite element method,” J. Mater. Eng. Perform., vol. 33, pp. 3731–3745, 2024.

24. Y. Fan, C. Yang, and Z. Hao, “Analysis of interfacial failure and particle damage of SiCp/Al with ultrasonic vibration-assisted cutting,” Eng. Fail. Anal., pp. 109225, 2024.

25. Y. Du, M. Lu, J. Lin, et al., “Experimental and simulation study of ultrasonic elliptical vibration cutting SiCp/Al composites: Chip formation and surface integrity study,” J. Mater. Res. Technol., vol. 22, pp. 1595–1609, 2023.

26. R. Muhammad, N. Ahmed, M. Demiral, et al., “Computational study of ultrasonically-assisted turning of Ti alloys,” Adv. Mater. Res., vol. 223, pp. 30–36, 2011.

27. J. Airao and C. K. Nirala, “Finite element modeling and experimental validation of tool wear in hot-ultrasonic-assisted turning of Nimonic 90,” J. Vib. Eng. Technol., vol. 11, pp. 3687–3705, 2023.

28. E. Saatçi, Y. F. Yapan, M. U. Uysal, et al., “Orthogonal turning of AISI 310S austenitic stainless steel under hybrid nanofluid-assisted MQL and a sustainability optimization using NSGA-II and TOPSIS,” Sustain. Mater. Technol., vol. 36, pp. e00628, 2023.